

**THE  $^{60}\text{Fe}$ - $^{60}\text{Ni}$  SYSTEMATICS OF UOC CHONDRULES, OPEN-SYSTEM REDISTRIBUTION COMPROMISES ITS USEFULNESS.** M. Telus<sup>1</sup>, G. R. Huss<sup>1</sup>, K. Nagashima<sup>1</sup>, R. C. Oglione<sup>1</sup>, <sup>1</sup>HIGP, University of Hawai'i at Mānoa, Honolulu, HI, USA. Email: [telus@higp.hawaii.edu](mailto:telus@higp.hawaii.edu).

**Introduction:** The  $^{60}\text{Fe}$ - $^{60}\text{Ni}$  short-lived radionuclide system has attracted attention because it potentially provides constraints on the stellar source of SLRs. Also, its relatively short half-life ( $t_{1/2}=2.6$  Myr) and the abundance of Fe in many chondritic components makes it a potentially powerful tool for early solar system chronology. Applying the  $^{60}\text{Fe}$ - $^{60}\text{Ni}$  system for these purposes has been severely hindered by discrepancies between initial  $^{60}\text{Fe}/^{56}\text{Fe}$  ratios inferred from bulk and *in situ* SIMS analyses. Here we discuss our SIMS analyses of chondrules from unequilibrated ordinary chondrites (UOCs) in the context of synchrotron X-ray fluorescence (XRF) measurements of those chondrules. We show that most chondrules behaved as open systems for Fe and Ni and may not be suitable for dating using the  $^{60}\text{Fe}$ - $^{60}\text{Ni}$  system or for constraining the initial  $^{60}\text{Fe}/^{56}\text{Fe}$  ratio of the solar system.

We historically assumed that since UOCs are the least thermally metamorphosed chondrites, the Fe-Ni system remained closed since the chondrules formed. However, synchrotron XRF analyses indicate that UOC chondrules have experienced extensive Fe-Ni mobility that was facilitated by fluid flow [1]. Evidence includes Fe and Ni enrichments in fractures at every scale (Figs. 1 & 2). SIMS spot analyses can easily overlap extraneous Fe and Ni, compromising the isotopic analyses. Here, we discuss the isotope measurements for three chondrules from Semarkona (LL3.00), Bishunpur (LL3.1/3.15), and Krymka (LL3.2) that show evidence for excess  $^{60}\text{Ni}$  and the influence of Fe-Ni mobilization on the isotopic data.

**Semarkona DAP-1** is a ~1 mm bleached radial-pyroxene chondrule with sulfide stringers that stretch across the entire length of the chondrule. For our SIMS analyses, we targeted areas between sulfide stringers. The bleached regions are fairly obvious and easy to avoid. Iron-Ni isotopic data for DAP-1 were collected during three separate sessions (March 2010, July 2010 and September 2011). An initial  $^{60}\text{Fe}/^{56}\text{Fe}$  ratio of  $\sim 2 \times 10^{-7}$  is inferred from these analyses ( $< 2.6 \times 10^{-7}$  (March),  $< 1.6 \times 10^{-7}$  (July), and  $(1.9 \pm 0.6) \times 10^{-7}$  (Sept)). In every case, excesses in  $^{60}\text{Ni}$  do not correlate well with the Fe/Ni ratio (e.g.,  $\chi_v^2=9$ ). Synchrotron XRF maps show that many of our SIMS spots overlap Ni-poor and Ni-rich sulfide. Some of these sulfides are probably secondary, which would explain the poor correlation between excess  $^{60}\text{Ni}$  and Fe/Ni ratio.

**Krymka chondrule KRM ch11** is a large (>1 mm) cryptocrystalline pyroxene chondrule that was analyzed in Dec. 2008 and July 2011. The initial ratio

inferred for this chondrule is  $\sim 2.6 \times 10^{-7}$ ,  $(2.3 \pm 1.8) \times 10^{-7}$  and  $\chi_v^2$  of 1.3 (Dec) and  $(2.9 \pm 2.1) \times 10^{-7}$  and  $\chi_v^2$  of 3.4 (July). Synchrotron XRF maps of this chondrule indicate extensive Fe-Ni mobilization along fine fractures, which many of our SIMS spots overlap (Fig. 1).

**Bishunpur chondrule BM80 ch13** is a porphyritic olivine and pyroxene chondrule (~750  $\mu\text{m}$  across). We measured both olivine and pyroxene. The initial  $^{60}\text{Fe}/^{56}\text{Fe}$  ratio inferred for this chondrule is  $(1.8 \pm 0.9) \times 10^{-7}$ , with a  $\chi_v^2$  of 5.6. Figure 2 shows the backscattered electron image, SIMS data and XRF maps of this chondrule. The X-ray maps show that some of our SIMS analyses were compromised by extraneous Fe-Ni rich material. In particular, the low Fe/Ni ratios of spots 1-4 may be due to overlap of SIMS analyses with extraneous Fe-Ni rich material.

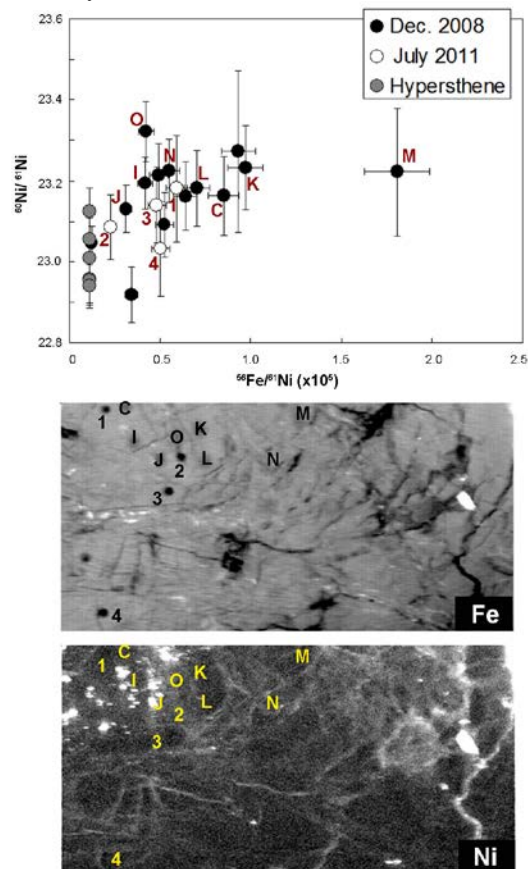


**Figure 1.** SIMS isotope analyses and Fe and Ni XRF maps for a cryptocrystalline pyroxene chondrule from Krymka KRM ch11. Spot analyses overlap Fe-Ni rich extraneous material in the chondrule fractures. Spots are labeled on the isochron as well as on the X-ray maps for comparison.

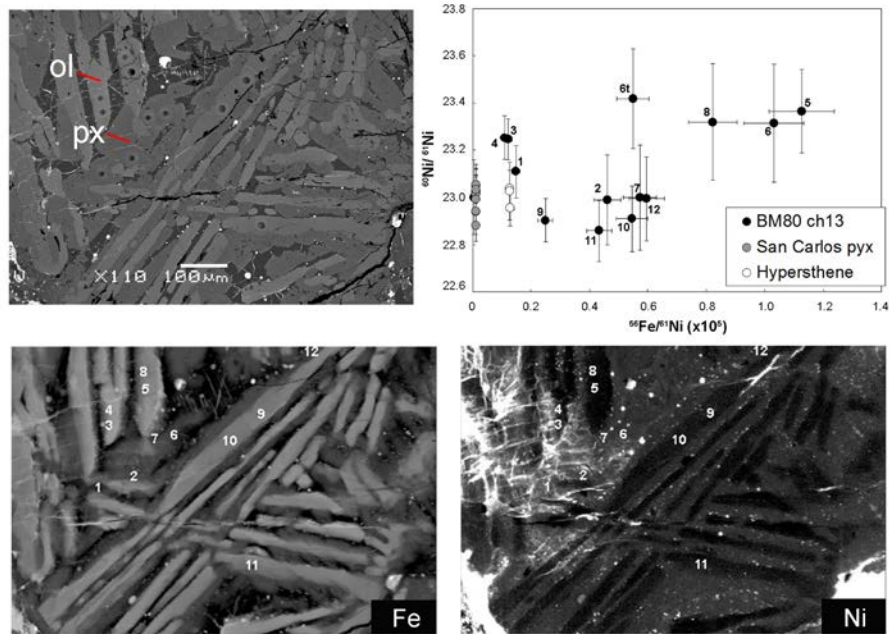


**Figure 2.** Backscattered electron image of porphyritic olivine (ol) and pyroxene (px) Bishunpur chondrule BM80 ch13 along with Fe and Ni XRF maps and SIMS isotopic data. Dark small circles in BSE are from SIMS analyses. The spot analyses are labeled on the Fe and Ni maps and on the isochron for comparison (analyses 6t and 6 were made in the same spot). Spots 1-4 clearly overlap extraneous Fe-Ni, which seems to come from the matrix.

**Discussion:** We have analyzed 25+ UOC chondrules over the past few years to constrain the initial  $^{60}\text{Fe}/^{56}\text{Fe}$  ratio of the solar system. Even though the Ni content in chondrule olivine and pyroxene is low ( $< 100$  ppm), most chondrules give initial ratios unresolved from zero. Many have upper limits of  $(0.5\text{--}2)\times 10^{-7}$ . A few chondrules have initial  $^{60}\text{Fe}/^{56}\text{Fe}$  ratios of  $(1\text{--}3)\times 10^{-7}$ . Our results are generally consistent with those of other SIMS groups [2-3]. But SIMS can give initial ratios more than an order of magnitude higher than those inferred from bulk analyses [4-6].

Open system redistribution of Fe and Ni is the likely source of the discrepancies between *in situ* and bulk analyses. Our synchrotron analyses show clear evidence for Fe-Ni enrichment along the chondrule fractures in all UOCs studied, including Semarkona, the least metamorphosed ordinary chondrite. Iron-Ni mobility was likely facilitated by fluid transport along grain boundaries and fractures on the chondrite parent body and/or during terrestrial weathering. During fluid transport, the chondrule exchanges Fe and Ni with the surrounding matrix, generally with a net gain of Fe and Ni, via fractures in the chondrules. This lowers both the measured excess of  $^{60}\text{Ni}$  and the Fe/Ni ratio for the chondrule. Bulk ICPMS and TIMS measurements likely incorporate this introduced Fe and Ni, even after leaching, resulting in erroneously low inferred  $^{60}\text{Fe}/^{56}\text{Fe}$  initial ratios. *In situ* analyses may be less influenced by extraneous Fe and Ni because large chondrule fractures can be avoided. But the poor corre-

lation between excess  $^{60}\text{Ni}$  and the Fe/Ni ratios for chondrules that have resolved initial  $^{60}\text{Fe}/^{56}\text{Fe}$  ratios shows that *in situ* measurements are also affected. Fine chondrule fractures are difficult to avoid with 20-40  $\mu\text{m}$  beam spots. If a meteorite experienced high temperatures, lattice diffusion may also affect the isotopic data. Mobilized Ni may diffuse out from olivine and pyroxene and into metal or sulfide due to the partition coefficients. Extracting Ni from olivine and pyroxene increases their Fe/Ni ratios, while exchange of Ni between Fe-silicates and metal/sulfide will lower the  $^{60}\text{Ni}$  excesses. Finding a chondrule that has not experienced either fluid-assisted Fe-Ni exchange or thermally driven diffusion will be challenging, but will be necessary in order to get reliable  $^{60}\text{Fe}$ - $^{60}\text{Ni}$  data.

**Conclusions:** The pervasive nature of Fe-Ni enrichment along chondrule fractures in UOCs indicates that these samples may not be suitable for constraining the initial  $^{60}\text{Fe}/^{56}\text{Fe}$  of the solar system. Other types of meteorites may provide better constraints. However, each sample needs to be characterized in detail, especially with regards to Fe and Ni redistribution.

**References:** [1] Telus M. et al. (2014) LPSC XLV, #2559. [2] Mishra R.K. and Chaussidon M. (2014) *EPSL* 398, 90-100. [3] Mishra R.K. and Goswami J.N. (2014) *GCA* 132, 440-457. [4] Chen J.H. et al. (2013) LPSC XLIV #2649. [5] Spivak-Birndorf L.J. et al. (2012) *MAPS*, 47, #5365. [6] Tang H. and Dauphas N. (2012) *EPSL*, 359, 248-263.

Supported by NASA NNX11AN62H (MT) and NNX11AG78G and NNX14AI19G (GRH).